

Heat Transfer and Bubble Movement of Two-Side and One-Side Heating Subcooled Flow Boiling in Vertical Narrow Channels

Liang-Ming Pan

Institute of Engineering Thermophysics of Chongqing University,
Chongqing 400044, China

Tien-Chien Jen

Mechanical Engineering Department,
University of Wisconsin at Milwaukee,
Milwaukee, WI 53211
e-mail: jent@uwm.edu

Chuan He

Ming-dao Xin

Institute of Engineering Thermophysics of Chongqing University,
Chongqing 400044, China

Qing-hua Chen

Mechanical Engineering Department,
University of Wisconsin at Milwaukee,
Milwaukee, WI 53211

This paper investigates the bubble behavior of different heating methods of narrow rectangular channels. Comparisons were made on the onset of nucleate boiling (ONB) point and bubble behavior with various flow patterns. Results reveal that the wall superheat of two-side heating is lower than that in one-side heating at the same heat flux. This difference becomes obvious at a higher heat flux. Under the same subcooling condition, the required heat flux to start nucleate boiling for the one-side heating channel is higher than that for the two-side one. With similar bubbles behaviors, the cross-sectional subcooling tends to be higher for the two-side heating method. [DOI: 10.1115/1.2227040]

Keywords: subcooled flow boiling, bubble behavior, two-side heating, one-side heating, narrow channels

1 Introduction

The channels employing hydraulic diameters between 200 μm and 3 mm are referred to as minichannels [1]. Compared with conventional channels from the view of the heat transfer, narrow and microchannels have significant heat transfer enhancement characteristics [2,3]. With a smooth internal surface and scouring by flowing fluid, the dirt formed on the surface of the channel wall can be easily removed and the fouling problem is not as serious as the deformed channels. Moreover, heat transfer elements can be easily assembled to compact devices. Since the innovative work of Ishibashi et al. [2], narrow channels have been adopted extensively in engineering applications, e.g., microelectronic cooling [4,5], advanced nuclear reactor [6,7], cryogenic, aviation, and space technology. Because the bubble size has approached the dimension of the channel, the size of the flow channel plays a critical role on the flow boiling heat transfer. This results in that the bubble in the narrow channel acts very differently from those in the non-narrow channel.

Yoshida et al. [8,9] studied the heat transfer performance of working media in a single-tube and double-tube thermosyphon, and investigated the effects of subcooling and inclination. They found that the performances of thermosyphon in single-tube and double-tube are quite different in the heat transfer rate and flow pattern. The effects of the heating methods on the parallel channel should be similar to the situation of a thermosyphon. However, there is no direct evidence about the comparison of bubble behavior dynamics of flow boiling in narrow channels between the one-side and the two-side heating situation.

During long historical practices of narrow channel investigation, a large number of experimental data and analytical results about one-side heating have been accumulated [10–12]. There are essentially no sufficient data available in the literature regarding the two-side heating for narrow channels. It will be very convenient if these one-side heating narrow channel data can be used to correlate and predict the two-side heating narrow channel transport phenomena and two-phase heat transfer performances.

For this reason, understanding the difference and similarity between these two heating methods (one-side heating and two-side heating) of the narrow channels are an essential task to develop the correlations. The feasibility of correlating the bubble behavior characteristics and boiling heat transfer features of one-side heating to two-side heating in narrow channels provides a convenient way to understand the inherent mechanism of heat transfer enhancement of narrow channels.

In the present work, we have experimentally compared the bubble behavior under the condition of one-side heating with that of two-side heating. Experimental studies are performed separately for a single plate heater system and a double plate heater system. A high-speed camera was used to compare the character-

Contributed by the Heat Transfer Division of ASME for publication in the JOURNAL OF HEAT TRANSFER. Manuscript received June 9, 2005; final manuscript received March 8, 2006. Review conducted by Sathish G. Kandlikar.

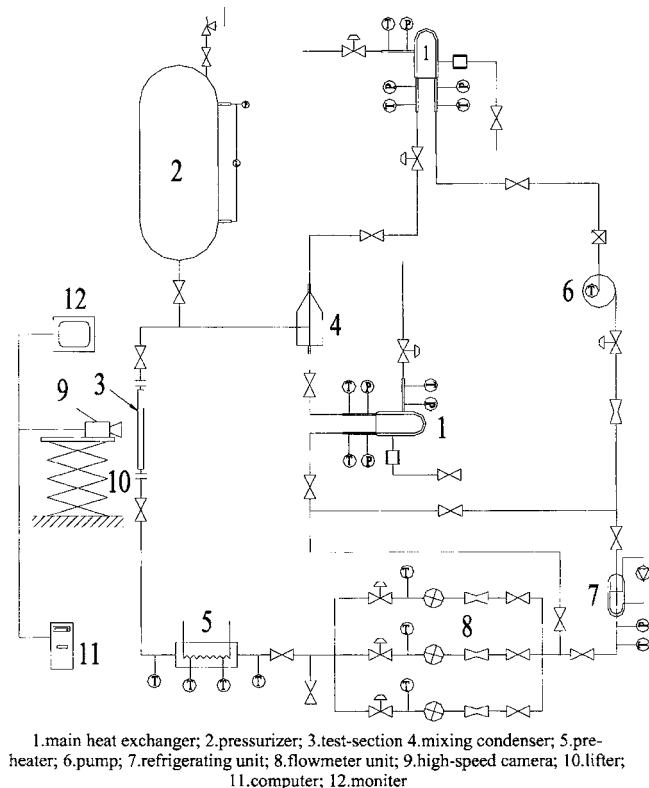


Fig. 1 Schematic diagram of test loop of R12

istics of bubble behavior. The onset of nucleate boiling (ONB) point and characteristics of the heat transfer of the narrow channel are also discussed.

2 Experimental Set-up and Data Treatment

2.1 Testing Apparatus for R12. Figure 1 is the schematic diagram of the complete experimental setup for the test loops and flow visualization. The test loop consists of a main test loop, water-cooling loop, power supply, control system, and other auxiliary systems. The test-loop unit consists of a main circulating pump, refrigerating unit, preheater, test section, condenser, heat exchanger, pressurizer, and flowmeter. Working fluid comes from pump 6 and then enters refrigerating unit 7, where it is refrigerated to the desired temperature if necessary. The flow rate is measured by the flowmeter with three different ranges of flow rates, and then working fluid enters the preheater to adjust the temperature to a designated temperature. After that, liquid is heated in test section 3 (details can be seen in Fig. 2). Then the two-phase flow enters condenser 4 to mix with the liquid directly coming from the pump. After cooling, the liquid flows back to the pump. The inlet temperature of the test section is controlled by a preheater and a refrigeration unit. The accuracy of the direct current power supply is $\pm 0.8\%$. The mass flow rate is measured by a venturimeter with an accuracy of $\pm 1\%$ of the whole measuring range of 50–500 kg/h. Pressure and pressure difference are measured by the pressure transmitter with a FOUNDATION™ fieldbus model STG960 (accuracy of ± 30 kPa) and pressure difference transmitter model ST3000 (Honeywell, accuracy of ± 3500 Pa). The temperature is measured from a T-type sheathed thermocouple. Every sheathed thermocouple is calibrated individually and the temperature measurement error of all the thermocouples is less than 0.45°C . The error distribution of the whole measuring range was accounted for in the data acquisition system. And all the thermocouples are located at a distance of at least of 100 mm from the inlet header tank. To avoid the inlet effect, the ONB points can

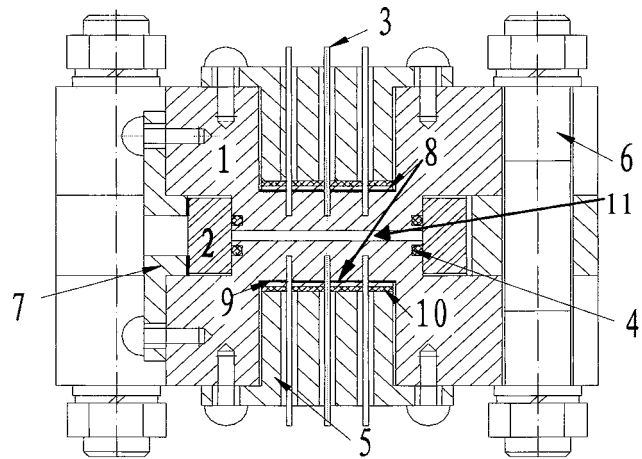


Fig. 2 Cross-sectional view of test section

often be adjusted to more than 160 mm downstream. The IMP distributed data acquisition system is used to obtain various signals from the test loop and test section at the accuracy of 0.03%. Besides, with good insulation outside the test section, the heat loss is only up to 1%. With careful heat loss calibration before every formal experiment at the single-phase flow state, the heat loss is taken into account in the final data processing. The calibration process based on the conservation of thermal energy is used to compare the outlet enthalpy with the combination of the inlet enthalpy plus the power input to the liquid.

2.2 Data Treatment and Parameters' Range. Since a flat heating element is used, numerical simulation is first performed to confirm that the heat flux distribution is uniform along the heating side. As shown in Fig. 2, three thermocouples are installed at the same height in one channel plate. Comparisons between the measured temperatures of distributed location and the simulation data confirm the uniformity of the heat flux distribution. The channel plates are made of brass (70Cu-30Zn) which has a thermal conductivity of 115 W/mK at room temperature. Since it is subcooled boiling, with the assumption of quasi-equilibrium within every cross section, the mean temperature of the flow can be evaluated from a simple energy balance on a differential length. The wall temperature can then be evaluated as follows

$$T_w = T_i - \frac{q\Delta x}{k} \quad (1)$$

in which, Δx is the distance from the measuring point to the channel wall, which is due to the fact that the inserting location is inside the wall (not right on the surface). T_i is the measured temperature, T_w is the calculated channel wall temperature. k is the thermal conductivity of the brass channel plates, in which the effect of the temperature dependence is taken into consideration. q is the heat flux with which the heat loss has been accounted for.

The experimental setting of the present work is: the heating length of the test section is 400 mm, the cross section of the channel is 35 mm in width and 2 mm in gap size, the mass flux varies between 700 and 1500 kg/(m²s), the heat flux and the pressure are ranging from 25 to 70 kW/m² and 1.3 to 2.0 MPa, respectively. Note that the heat flux is defined as the heat transfer rate per unit heating area. The subcooled boiling condition is maintained by limiting the power input of the test section according to the inlet enthalpy. There is no extra measure used to preserve the subcooled flow. The pressure is defined as the average

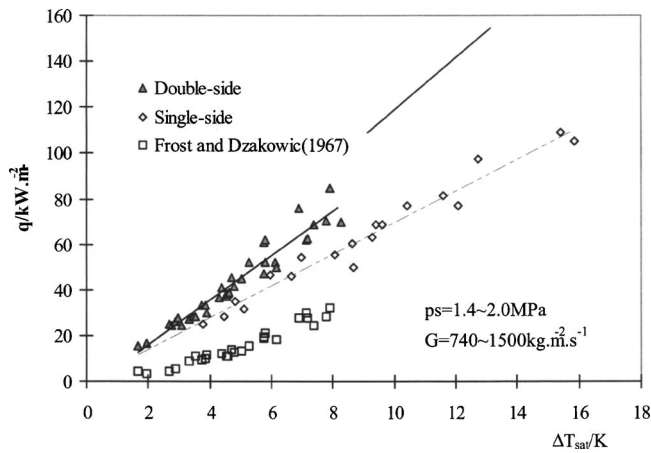


Fig. 3 Wall superheat versus the ONB point of one-side and two-side heating as well as the prediction of Frost and Dzakowic (see Ref. [18])

absolute pressure of the inlet and the outlet. The pressure is used as a reference to calculate the saturated temperature and other physical properties according to the computer code of NIST REFPROP (1992 Version, new version can be found at <http://www.nist.gov>). There are a total of 48 thermocouples used in the experiment to measure the temperatures of the test section with 24 thermocouples on each of the heating walls.

3 Experimental Procedures and Results Discussion

3.1 Experimental Method. Before the start of the experiment, careful calibration is performed to ensure the test equipment is ready. The pressurizer in the test loop is first started to increase the pressure to the desired value, then the main loop and the R-12 preheating equipment are used to adjust the flow rate and the inlet temperature to the desired value. The heating power supplied to the test section is increased gradually until the outlet temperature reaches the saturated boiling point, and then waits for a couple of minutes until all the parameters of every measuring point have no change within the accuracy of the measuring instruments. Then the temperature of all points of the test section is measured and the location of the ONB point of subcooled boiling is recorded. Meanwhile, a high-speed video camera is started to take images. After the two-side heating experimental data are recorded, one of the two heaters in Fig. 2 is cutoff to perform the one-side heating experiment with the same system parameters. Since two-phase flows are inherently unsteady, 50 samples per channel are obtained over a period of 0.5 s and averaged to achieve repeatable measurements. Under various operating conditions, 97 runs of two-side and one-side heating experiments are performed, and a large number of high-speed video images are recorded as well.

3.2 Effect of Heating Method on the ONB Point. The ONB point is a key transition point for the boiling heat transfer, and a critical point to adopt different correlations for the rate of the heat transfer.

The ONB points are determined by using high-speed video. According to the temperature of the heating wall as well as system parameters, the relationship between the subcooled ONB point and the wall superheat for one-side and two-side heating is shown in Fig. 3 with a system pressure $p_s = 1.4\text{--}2.0$ MPa and mass flux $G = 740\text{--}1500$ kg/m² s. The average subcooling of the ONB point in one-side and two-side heating is shown in Fig. 4 with a constant mass flux at $G = 1500$ kg/m² s. In these figures, the average subcooling is defined as the difference between the current cross-sectional temperature (calculated through thermal energy balance) and the saturated temperature at the present pressure. The heat flux is defined as the following

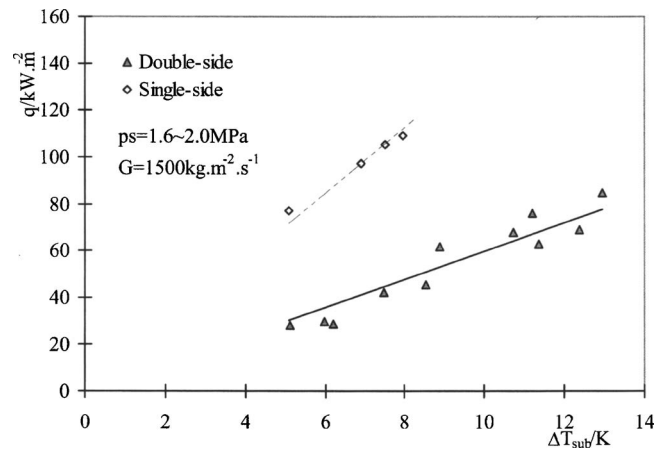


Fig. 4 Subcooling of liquid versus the ONB point of one-side and two-side heating

$$q = \frac{P}{A_{ha}} \quad (2)$$

in which P is the electric power input into the heating plate(s), (kW) and A_{ha} is the total heating area (m²).

In Fig. 3, it can be seen that the different heating methods (one-side heating or two-side heating) have apparent effects on the subcooled ONB point and the wall superheat. With the same heat

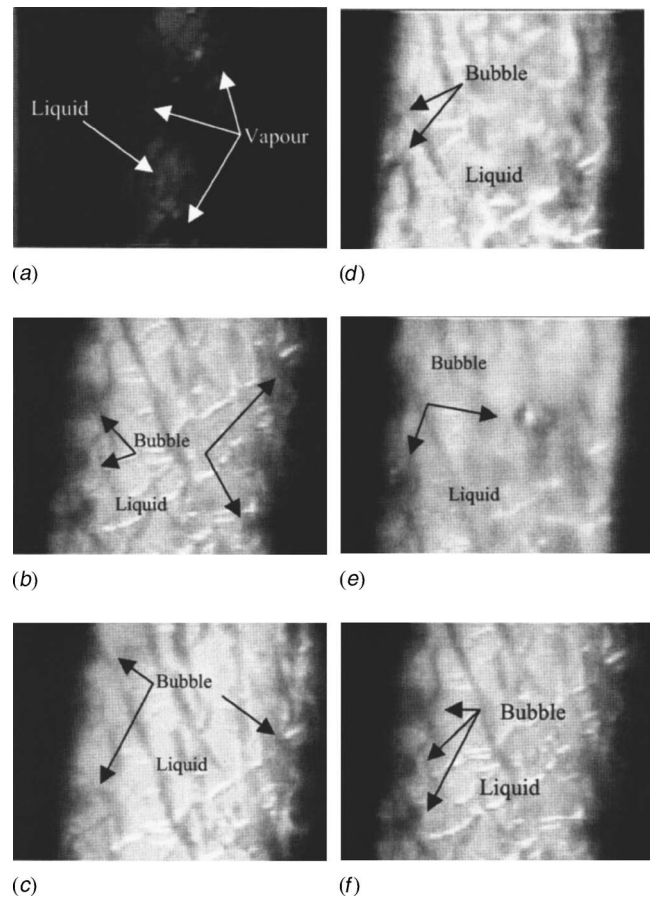


Fig. 5 Bubble morphology in different heating conditions: (a) two-side heating, (b) one-side heating, (c) two-side heating, (d) one-side heating, (e) two-side heating, and (f) one-side heating

Table 1 Experimental conditions of Fig. 5

No.	p/MPa	$G/\text{kg m}^{-2}$ s^{-1}	q/kW m^{-2}	$v/\text{m s}^{-1}$	x_{out}	ΔT_{sub} K	Bubble description
5(a)	2.03	648.5	27.8	0.8	0.064	3.22	Liquid bridge was formed, bubbles filled half channel
5(b)	2.01	678.0	24.8	0.312	-0.018	6.44	Big bubbles coalesced small bubbles, which size increased
5(c)	1.81	812.7	28.0	0.291	0.036	6.18	Have big bubbles, in discrete moving
5(d)	1.81	800.7	28.2	0.278	-0.019	7.06	Moving discrete bubbles
5(e)	1.83	1059.4	38.7	0.3	0.022	8.21	Rolling moving, bigger bubbles move faster and coalesced small bubbles on rolling away
5(f)	1.82	1170.4	34.7	0.86	-0.026	4.01	Bubbles are very big, and the amount is few

flux input, the wall superheat of the subcooled ONB point in the two-side heating channel is less than that in one-side heating. This effect is more pronounced when the heat flux is further increased.

The reason of the increasing difference in the wall superheat phenomenon could be explained as follows: under the condition of two-side heating, the disturbances of the bubble were largely enhanced between both heating walls, which resulted in decreasing the wall superheat. This is similar to the heat transfer enhancement in narrow channels [2,13]. Comparing the two groups of the present experimental data with the correlation of Frost and Dzakowic [14] (which was extended from Davis and Anderson's [15] analytical solution to cover liquids other than high pressure water flows) at the same system parameter of two-side heating shows that the ΔT_{sup} is much higher in Frost and Dzakowic [14] than the experimental data for the two heating methods in the present study. This result also suggests that two-side heating has a lower superheat than the one-side heating case.

Comparing to the one-side and two-side heating cases, it can be seen from Fig. 4 that the heat flux for the onset of boiling is quite different under the same condition of subcooling. The heat flux required by the onset of boiling in the two-side heating channel is much less than that in one-side heating. With decreasing subcooling of the cross section, these two curves tend to approach each other. The reason for a different ONB heat flux between the two cases is due to the development of the two thermal boundary layers of both sides under the condition of two-side heating, which makes the ONB point shift to up-stream. With increasing heat flux, the disturbance between the two thermal boundary layers is enhanced, and the ONB point will shift further up-stream.

As described above, one-side and two-side heating have strong effects on the ONB point. Under the same operating conditions, the ONB is quite different when a different heating method is used. When the ONB point is considered, the two-side method of subcooled flow boiling cannot be simply simulated under the one-side heating condition.

3.3 Bubble Morphology in Different Heating Conditions.

For bubble morphology, it will be shown that the one-side heating method is quite different from the two-side heating method. As shown in Fig. 5, under approximately the same pressure, mass flow rate, heat flux, and average subcooling of cross-sectional conditions (see Table 1 for the operation conditions for Fig. 5), the bubble behavior displays many differences between the two heating methods.

Figures 5(a) and 5(b) illustrate the photoimages of the cases for two-side heating and one-side heating, respectively, under almost identical conditions (see Table 1). It can be seen from Fig. 5(a) that the channel was filled with a large amount of bubbles and the liquid only existed as a liquid bridge. On the contrary, as shown in Fig. 5(b), in one-side heating, only a few isolated bubbles scattered on the heating surface.

Similarly, Figs. 5(c) and 5(d) depict the photoimages for two-side heating and one-side heating, respectively, with a larger mass and heat flux, and slightly lower system pressure (see Table 1). Comparing Fig. 5(c) to Fig. 5(d), it can be observed that with two-side heating (Fig. 5(c)), the number of bubbles on the heating

surface is larger than that of one-side heating (Fig. 5(d)).

Figures 5(e) and 5(f) show the images of the cases for two-side heating and one-side heating at a higher mass flux and wall heat flux (see Table 1), respectively. The difference of the working condition between them is mainly the subcooled temperature of the cross section, which are the 8.21 K for two-side heating and 4.01 K for the one-side heating. It is observed that the bubble morphology is very similar; both cases have big bubbles, and the bubbles are all rolling downstream. This implies that the two different heating methods have resulted in the same bubble morphology at a different subcooled temperature. When we do not consider the operational conditions other than flow patterns, the difference of the bubbles behavior between the two heating methods is not easy to be distinguished. Thus the results of the different heating methods are dominantly reflected on the subcooling of the cross-sectional liquid and wall superheat. This indicates that the differences of the behaviors of the bubbles are unapparent if we do not consider the relevant conditions.

From the working parameters of the photoimages, it can be seen that when the bubble morphology is similar, the subcooling of the section is higher for the two-side heating method. Meanwhile, under the situation of similar bubble morphology, bubbles will move at a higher speed for the one-side heating method than those at the two-side heating method. This mechanism can be explained as follows: under the condition of subcooled boiling, fluid near the nonheating wall of the one-side heating is a single-phase liquid, the friction is less than the one that has bubbles moving on the opposite heating wall.

4 Conclusion

(1) The heating methods of the narrow channels of two-side and one-side heating have strong effects on the wall superheat of the subcooled ONB point. At the same heat flux, the wall superheat under the condition of two-side heating is lower than that in one-side heating. When the heat flux is increased, the difference in the wall superheat between both cases is also increased.

(2) At the ONB point, under the same cross-sectional subcooling, the required heat flux to initiate nucleate boiling for the one-side heating narrow channel is higher than that for the two-side heating channel. By decreasing the cross-sectional subcooling, the difference narrows.

(3) When the operating conditions are nearly identical, the bubbles behavior in one-side and two-side heating is quite different as observed from the photoimages. Note that with similar bubbles behaviors, the cross-sectional subcooling tends to be higher for two-side heating cases.

Acknowledgment

The authors are grateful for the support of the National Science Foundation of China (No. 50406012) and the support of the National Key Laboratory of Bubble Physics and Natural Circulation, Nuclear Power Institute of China (No. 51482020103JW2001). Dr. Tien-Chien Jen and Qinghua Chen would also like to acknowledge the partial support from NSF (US) DMII GOALI 9908324.

Nomenclature

- A_{ha} = heating area, m^2
 k = thermal conductivity of materials, $W\ m^{-1}\ K^{-1}$
 p = pressure, MPa
 P = electric power input into the heating plate(s), kW,
 G = mass flux of R-12, $kg\ m^{-2}\ s^{-1}$
 q = heat flux, $kW\ m^{-2}$
 T_i = temperature of the measuring point, K
 T_w = temperature of channel wall, K
 x_{out} = mass dryness fraction of outlet,
 $(H_{out} - H_{sat})/H_{sat}$
 Δx = distance from measuring point to channel wall, m
 ΔT_{sub} = subcooled temperature of R-12, $\Delta T_{sub} = T_{sat} - T$, K
 ΔT_{sup} = superheated temperature of heating wall, $\Delta T_{sup} = T_w - T_{sat}$, K
 v = velocity of bubbles, $m\ s^{-1}$

References

- [1] Kandlikar, S. G., 2002, "Fundamental Issues Related to Flow Boiling in Minichannels and Microchannels," *Exp. Therm. Fluid Sci.*, **26**, pp. 389–407.
[2] Ishibashi, E., and Nishikawa, K., 1969, "Saturated Boiling Heat Transfer in Narrow Spaces," *Int. J. Heat Mass Transfer*, **12**, pp. 863–894.
[3] Yao, S. C., and Chang, Y., 1983, "Pool Boiling Heat Transfer in a Confined Space," *Int. J. Heat Mass Transfer*, **26**(6), pp. 841–848.
[4] Mukherjee, S., and Mudawar, I., 2003, "Smart Pumpless Loop for Micro-Channel Electronic Cooling Using Flat and Enhanced Surfaces," *IEEE Trans. Compon. Packag. Technol.*, **26**(1), pp. 99–109.
[5] Misale, M., and Bergles, A. E., 1997, "Influence of Channel Width on Natural Convection and Boiling Heat Transfer From Simulated Microelectronic Components," *Exp. Therm. Fluid Sci.*, **14**(2), pp. 187–193.
[6] Larson, T. K., Oh, C. H., and Chapman, J. C., 1994, "Flooding in a Thin Rectangular Slit Geometry Representative of ATR Fuel Assembly Side-Plate Flow Channels," *Nucl. Eng. Des.*, **152**(2), pp. 277–285.
[7] Ruggles, A. E., 1990, "Countercurrent Flow in Systems of Parallel Narrow Rectangular Channels," *Proc. of Advances in Gas-Liquid Flows, ASME Winter Annual Meeting*, pp. 243–250.
[8] Yoshida, M., Imura, H., and Ippohshi, S., 1993, "Flow and Heat Transfer in Two-Phase Double-Tube Thermosyphons (the Effect of Subcooling)," *Heat Transfer-Jpn. Res.*, **22**(8), pp. 812–827.
[9] Imura, H., and Yoshida, M., 1991, "Heat-Transfer Characteristics in Two-Phase Double-Tube Thermosyphons," *Heat Transfer-Jpn. Res.*, **20**(8), pp. 723–733.
[10] Boscary, J., Fabre, J., and Schlosser, J., 1999, "Critical Heat Flux of Water Subcooled Flow in One-Side Heated Swirl Tubes," *Int. J. Heat Mass Transfer*, **42**(2), pp. 287–301.
[11] Boscary, J., Araki, M., and Schlosser, J., 1998, "Dimensional Analysis of Critical Heat Flux in Subcooled Water Flow Under One-Side Heating Conditions for Fusion Application," *Fusion Eng. Des.*, **43**(2), pp. 147–171.
[12] Boyd, R. D., Sr., and Penrose, C., 2002, "Conjugate Heat Transfer Measurements in a Nonuniformly Heated Circular Flow Channel Under Flow Boiling Conditions," *Int. J. Heat Mass Transfer*, **45**(8), pp. 1605–1613.
[13] Bowers, M. B., and Mudawar, I., 1994, "High Flux Boiling in Low Flow Rate, Low Pressure Drop Mini-Channel and Micro-Channel Heat Sinks," *Int. J. Heat Mass Transfer*, **37**, pp. 321–332.
[14] Frost, W., and Dzakowic, G. S., 1967, "An Extension of the Method of Predicting Incipient Boiling on Commercially Finished Surfaces," *ASME AICHE Heat Transfer Conference Paper 67-HT-61*, Seattle; <http://wins.engr.wisc.edu/teaching/mpfBook/node35.html>.
[15] Tong, L. S., and Tang, Y. S., 1997, *Boiling Heat Transfer and Two-Phase Flow*, Taylor & Francis, Washington, D.C., p. 251; Davis, E. J., and Anderson, G. H., 1966, "The Incipience of Nucleate Boiling in Forced Convection Flow," *AIChE J.* **12**, pp. 774–780.